

Effect of Surge Current Testing on Reliability of Solid Tantalum Capacitors

Alexander Teverovsky

Perot Systems

Code 562, NASA GSFC, Greenbelt, MD 20771

Alexander.A.Teverovsky.1@gsfc.nasa.gov

I. Introduction.

Tantalum capacitors manufactured per military specifications (MIL-PRF-55365) are established reliability components and have less than 0.001% of failures per 1000 hours (the failure rate is less than 10 FIT) for grades D or S, thus positioning these parts among electronic components with the highest reliability characteristics. Still, failures of tantalum capacitors do happen and when it occurs it might have catastrophic consequences for the system. This is due to a short-circuit failure mode, which might be damaging to a power supply, and also to the capability of tantalum capacitors with manganese cathodes to self-ignite. During such a failure, a substantial amount of energy is released by exothermic reaction of the tantalum pellet with oxygen generated by the overheated manganese oxide cathode, resulting not only in destruction of the part, but also in damage of the board and surrounding components.

A risk of using of an electronic component, and a tantalum capacitor in particular, can be defined as a product of the probability of failure and consequences (expressed for example as the cost of rework, retesting, redesign, project delays, etc.). In this regard, tantalum capacitors can be considered as low failure rate parts with a high risk of application. To reduce this risk, further development of a screening and qualification system with special attention to the possible deficiencies in the existing procedures is necessary.

A specific feature of tantalum capacitors is so-called surge current or turn-on failures when the board is first powered up. The mechanism of surge current failures has not been understood completely yet, and different hypotheses were discussed in relevant literature. These include a sustained scintillation breakdown model [1-3]; electrical oscillations in circuits with a relatively high inductance [4-6]; local overheating of the cathode [5, 7, 8]; mechanical damage to tantalum pentoxide dielectric caused by the impact of MnO_2 crystals [1, 9, 10]; or stress-induced-generation of electron traps caused by electromagnetic forces developed during current spikes [11].

The existing system of screening and qualification of tantalum capacitors per MIL-PRF-55365 is supposed to assure that the parts would operate reliably at two operating environments: steady-state and surge current conditions. A so-called Weibull grading test, which is a version of a burn-in performed typically at 85 °C and voltages varying from 1.1VR to 1.53VR for up to 40 hours, is used to assure that reliability of the parts at steady-state conditions is below the required level. Surge current testing (SCT) is used to eliminate possible failures in applications under surge current conditions.

In spite of the obvious importance of SCT, this test is optional per MIL-PRF-55365. More than that, even its position in the manufacturing process, in particular, whether to perform it before (option C) or after (option B) Weibull grading or voltage ageing tests, is left to customer choice. Some customers believe that SCT might damage tantalum pentoxide dielectric, and hence this test should be carried out before the Weibull grading with the hope that the parts degraded by SCT would be screened out by burning in. One might also speculate that the long-term high-voltage stress at high temperatures might degrade the capability of capacitors to withstand surge current stresses, and thus the SCT should be carried out after Weibull grading. Unfortunately, neither of the opinions has been substantiated by adequate engineering analysis, and decisions are often made based on unverified data. The situation with the surge current screening is likely a reflection of uncertainty about the mechanism of failure and processes causing possible degradation of the parts. Also, there is only scarce experimental data on the effect of surge current events on the reliability of tantalum capacitors.

An attempt to evaluate the effect of the surge current testing on long-term reliability of the parts was performed by Sprague Electric under NASA contract NAS8-33424 more than 30 years ago [12]. However, the results were inconclusive due to a small number of failures. More recently [7], life testing of the capacitors after multiple, 10000 surge cycles at the rated voltage was performed and showed no detectable difference in results as compared to the reference samples.

The purpose of this work is evaluation of the effect of surge current stress testing on reliability of the parts at both steady-state and multiple surge current stress conditions. In order to reveal possible degradation and precipitate more failures, various part types were tested and stressed in the range of voltage and temperature conditions exceeding the specified limits. A model to estimate the probability of post-SCT-screening failures and measures to improve the effectiveness of the screening process has been suggested.

II. Experiment.

Ten different types of commercial tantalum capacitors have been used in this study. The part types selected represented components used in space applications, had high CV values varying from 525 $\mu\text{F-V}$ to 3300 $\mu\text{F-V}$, and had a relatively large size of 7343 per EIA size code.

A test setup used for SCT is shown in Figure 1. To increase the amplitude of surge current spike, no limiting resistors were used. Four power MOSFETs were connected in parallel and used to discharge a 13,600 μF bank capacitor (CB) onto the device under test (DUT). Oscillograms of the charge current spikes were monitored using a Tektronics AM503 current probe amplifier and a digital oscilloscope. A precision semiconductor analyzer, hp4156A, was used to provide current to charge CB, generate gate pulses to open the switch, and record the amplitudes of current spikes, applied voltages, and currents, I_c , at the end of the charging cycle. The program allowed for setting the number of surge cycles, N_c , initial test voltage, V_o , and voltage increments between the steps, ΔV , to carry out step stress surge current testing (3SCT), which typically begins with the rated voltage and continues until a failure occur. The failure event was detected automatically when post-spike and/or charging currents exceeded the set threshold values. After the failure is detected, the breakdown voltage and number of cycles to failure were recorded and the program stopped.

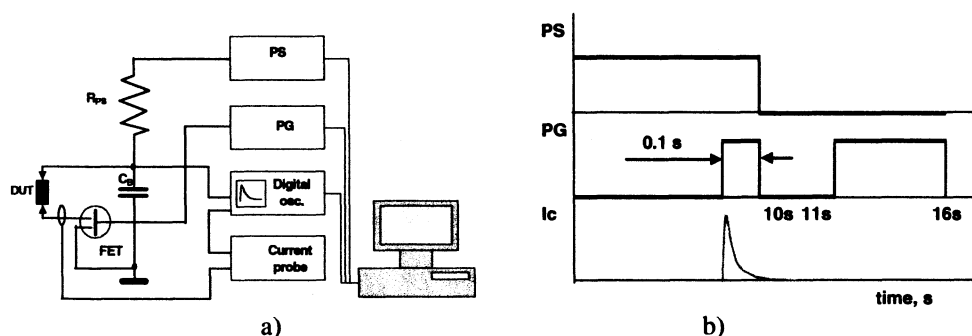


Figure 1. Test setup (a) and timing diagram (b) of the surge charge current testing.

Figure 2.a shows typical oscillograms observed during 3SCT of 220 $\mu\text{F}/6\text{V}$ capacitors. Based on these data, the amplitudes of current spikes, I_{sp} , were plotted against the applied voltage for several part types as shown in Figure 2.b. The results clearly indicate a linear relationship between I_{sp} and V , thus allowing calculation of the effective resistance, R_{eff} , of the surge current test circuit.

The value of R_{eff} was found to correlate with the ESR values of the tested capacitors. This indicates that the used setup does not introduce substantial additional impedance (active, caused by contacts and wires, or inductive, caused by the length of interconnections) to the circuit, and that the ESR value is a major contributor to the resistance of the circuit. The value of R_{eff} is important to characterize the setup used and is an effective means to assure proper, low-resistive contacts to the DUT and adequate operation of the SCT circuit.

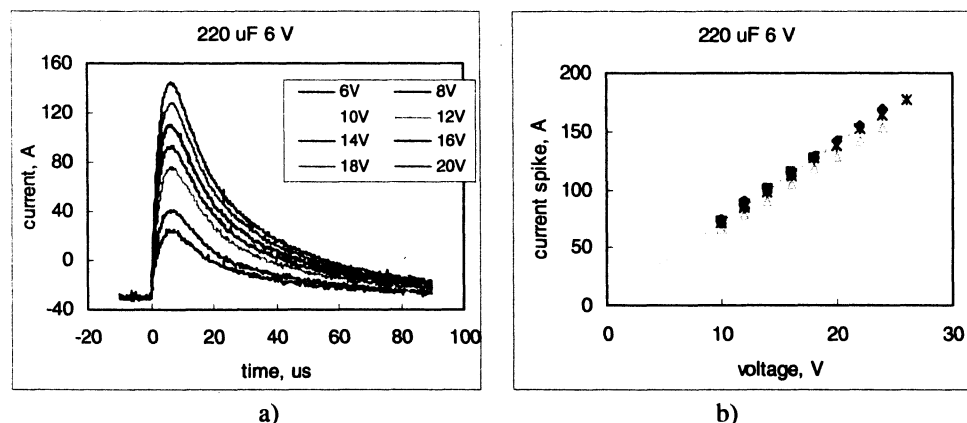


Figure 2. Current spikes in a 220 μ F 6 V capacitor (a), and variation of the amplitude with voltage for nine samples (b). The slope of the lines indicates the effective resistance, R_{eff} , which in this case had an average value of 149 milliohms and a standard deviation of 4 milliohms.

Results of 3SCT for the 10 part types showed that the characteristic breakdown voltages exceeded the rated voltages by two times on average. However, the spread of this ratio was large and varied from 1.2 to 3.6, resulting in a situation in which parts with a lower rated voltage had much higher breakdown voltages than parts rated to a higher voltage. This means that generally, the rated voltage is not an indicator of the robustness of the parts in surge current environments. The shape factors for VBR_3SCT distributions averaged 7.9 with a spread from 5.2 to 14.3. For some part types, bimodal Weibull distributions provided a better fit than unimodal distributions thus indicating the presence of low-voltage and high-voltage subgroups in the lot.

III. Effect of SCT on reliability under steady-state conditions.

III.1 Life test at 125 °C

A highly accelerated life test was performed at conditions similar to the Weibull test per MIL-PRF-55365. However, to precipitate more failures, the test temperature was increased from 85 °C to 125 °C, the stress voltage was 1.5*VR, and the failure current was reduced from 1 A to 2 A required per the MIL standard to 0.125 A. Note that the Weibull grading test is performed in the range of voltages from VR to 1.53*VR and results in acceleration factors varying at 85 °C from 1 to 20,000. Obviously, acceleration factor at 125 °C will be even greater, so a 100 hour test at 125 °C and $V = 1.5 VR$ would be equivalent to testing for more than 230 years at the rated voltage and 85 °C.

The parts intended for life testing were soldered onto FR4 boards in groups of 16 samples, and each capacitor was connected to a power supply through fast-acting fuses rated to 125 V and 125 mA. The nominal cold resistance of the fuses was 1 Ohm, which is in compliance with MIL-PRF-55365. The average time current curves for the fuses indicate that for pulses of less than ~ 1 ms, which are typically expected during failure events, the 125 mA fuses will blow at currents exceeding 0.8A. Note also, that employment of 2 A fuses per MIL-PRF-55365, at these conditions would result in failures only for parts experiencing spikes of more than ~ 15 A, whereas parts having spikes of a few amperes would not be detected and if their characteristics after the test are within the specified limits, these parts would be considered as acceptable.

A summary of life test results, including test conditions, quantity of failed parts, Weibull characteristics of the relevant life time distributions, and p-values of the Fisher exact test are shown in Table 1. The p-value indicates a statistical significance of difference between the proportions of failed parts. Typically, the difference can be considered as significant if $p < 0.05$. Analysis of the results indicates that SCT screening even at voltages of 1.5VR does not cause additional failures during 125 °C life testing. Interestingly, the values of the shape parameter, β , calculated in the assumption of unimodal Weibull distributions, were less than 1, indicating that most observed failures are infant mortality failures caused by some manufacturing-induced flaws in the part.

Table 1. Summary of life test results at 125 °C

Part	Life Test Condition	Precondition	QTY	Failures	Weibull Distr.		Fisher Exact
					η , hr.	β	
100 μ F/16 V	24V, 72 hr	w/o SCT	25	16	52.4	0.19	0.82
		SCT 16 V, 10c	25	19	5.6	0.27	
220 μ F/6 V	9V, 168 hr	w/o SCT	16	0	-	-	1
		SCT 9 V, 10c	16	1	-	-	
47 μ F/20 V Mfr. K	30V, 168 hr	w/o SCT	16	7	24102	0.13	0.74
		SCT 30 V, 10c	16	5	779	0.44	
33 μ F/35 V Mfr. A	50V, 250 hr	w/o SCT	16	10	1337	0.22	0.54
		SCT 50 V, 10c	16	6	8487	0.28	
33 μ F/35 V Mfr. K	50V, 168 hr	w/o SCT	16	6	3153	0.27	0.72
		SCT 50 V, 10c	16	4	65780	0.22	

III.2 Life test at room temperature.

This test was carried out by monitoring leakage currents at room temperature and $V = 2VR$ for up to 200 hours. Two subgroups of different part types, with 9 to 18 samples each, were used. To simulate SCT screening, one of the subgroups was stressed by multiple ($N_c = 10$ to 30) cycles at voltages in the range from 1.25VR to 2VR, and another was comprised of unscreened parts.

During RT life testing, the voltage was applied to each sample via a 1 kOhm resistor, and the currents were measured and recorded by a PC-based data-capturing system every 10 seconds. A failure event was detected and recorded when a scintillation current spike occurred. It was assumed that similar spikes caused failures during 125 °C life testing. However, contrary to room temperature testing, the currents during 125 °C testing were not limited with a resistor thus sustaining the breakdown and causing the fuse to blow.

Room temperature test results are summarized in Table 2. Similar to life testing at 125 °C, statistical analysis of the results showed no difference in the proportion of life test failures (scintillations) in parts stressed and non-stressed by surge current test screening.

Table 2. Summary of life test results at RT

Part	Life Test Condition	Precondition	QTY	Failures
100 μ F/16 V	32 V, 144 hr	w/o SCT	9	1
		SCT 20 V, 30c	9	0
220 μ F/6 V	12 V, 200 hr	w/o SCT	18	2
		SCT 12 V, 10c	18	3
47 μ F/20 V Mfr. K	40 V, 200 hr	w/o SCT	18	6
		SCT 40 V, 10c	9	3
47 μ F/20 V Mfr. A	40 V, 200 hr	w/o SCT	9	1
		SCT 30 V, 10c	9	0

IV. Effect of life testing on results of 3SCT.

To reveal a possible effect of life testing on surge current breakdown voltages, parts from seven different lots were subjected to 3SCT after life testing at 1.5VR and 125 °C and after long-term bias at room temperature. Average breakdown voltages and standard deviations measured during post-life 3SCT are presented in Table 3. For reference, the table shows also results obtained using unstressed devices.

Table 3. Summary of life test results at RT

Part	Condition	QTY	Average	STD
220 μ F/6 V	unstressed	36	19.85	4.52
	passed 168hr 125C 9V	16	20.62	2.6
	passed 168hr RT 12V	15	24.13	3.89
100 μ F/16 V	unstressed	29	27.99	6.31
	passed 125C 72hr 24V	10	28.80	5.90
	passed RT 144hr 32V	17	32.47	6.18
47 μ F/20 V, Mfr. K	unstressed	65	40.15	8.87
	passed 168hr 125C 30 V	20	41.60	6.64
	passed 200hr RT 40 V	15	46.80	8.37
47 μ F/20 V, Mfr. A	unstressed	23	33.29	5.38
	passed 200hr RT 30 V	17	40.82	5.56
33 μ F/35 V, Mfr. A	unstressed	25	66.38	7.20
	passed 250hr 125C 50V	8	66.12	13.79
33 μ F/35 V, Mfr. K	unstressed	28	71.96	5.77
	passed 168hr 125C 50V	14	71.43	9.25
15 μ F/35 V	unstressed	39	65.34	10.86
	passed 125hr RT 50 V	9	65.67	13.6

No significant effect of life testing at 125 °C was observed. However, long-term room temperature testing of 4 out of 5 part types (220 μ F/6 V, 100 μ F/16 V, 47 μ F/20 V, Mfr. K, and 47 μ F/20 V, Mfr. A) resulted in an increase of breakdown voltages on ~ 10 to 20%. Long-term RT testing of 15 μ F/35 V capacitors was carried out at 1.5VR and did not cause significant variations in VBR_3SCT.

Testing of the parts that failed life testing showed that their surge current breakdown voltages were similar to virgin parts, thus indicating that self-healed scintillation breakdowns likely do not degrade the capability of capacitors to withstand surge current conditions. However, parts that were capable of withstanding hundreds of hours of steady-state testing at 2VR, failed 3SCT at voltages much lower than 2VR. This suggests that the scintillation and surge current breakdowns probably have different mechanisms, and "proofing" of the parts does not guarantee their reliability under surge current conditions.

V. Failures during multiple surge current cycling.

To estimate the probability of failures at $N_c > 10$, several part types were subjected to 3SCT at multiple cycles at each voltage step. The current spike amplitude was used as an in-situ parameter indicating possible degradation in the parts. It was expected that surge-current-induced-stresses might increase ESR and/or leakage currents and thus degrade I_{sp} and increase R_{eff} .

A 100-cycle-per-step surge current test was carried out on 47 μ F/20 V, 330 μ F/10 V, 220 μ F/6 V, and 100 μ F/16 V capacitors. Typical examples of I_{sp} - N_c variations and dependencies of the slope on the stress voltages for 47 μ F/20 V capacitors are presented in Figure 3. Similar results were obtained for other part types and show that even at voltages that cause breakdown after multiple cycling, there was no systematic variation of the amplitude of current spike with the number of cycles.

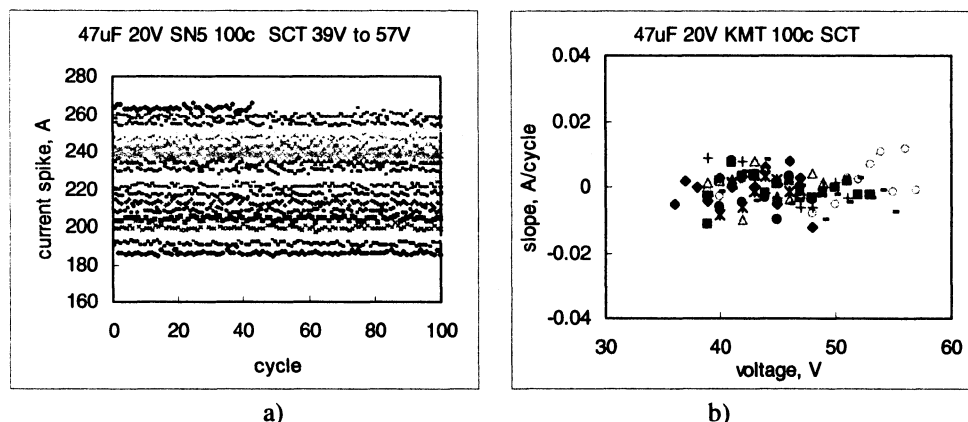


Figure 3. Variations of current spike amplitudes for a 47 $\mu\text{F}/20\text{ V}$ capacitor with the number of cycles during 3SCT starting from 39 V in 1 V increments (a), and dependence of the slope on stress voltage during 100-cycle testing of 9 samples. Note that SN5, Figure (a), failed cycle 43 at 57 V.

Results of 10- and 100-cycle-per-step 3SCT at $\Delta V = 1\text{ V}$ for 220 $\mu\text{F}/6\text{ V}$ capacitors are shown in Table 4. During this test ~53 % of parts failed at first cycle during 10-cycle test, whereas only 20 % failed at first cycle after passing 100 cycles at a voltage only 1 V lower than the breakdown voltage. Seven out of 10 parts failed at N_f more than 10. The number of cycles to failure in the rest of the group apparently varied randomly from 1 to 99 cycles, without correlation to V_{BR_3SCT} .

Table 4. Failure conditions of 220 $\mu\text{F}/6\text{ V}$ capacitors during 10- and 100-cycle-per-step 3SCT in 1 V increments.

	10 cycles in 1V incr.		100 cycles in 1V incr.	
	V_{BR_3SCT}	cycle	V_{BR_3SCT}	cycle
SN1	19	3	19	31
SN2	18	6	20	14
SN3	20	1	21	1
SN4	22	4	23	99
SN5	19	1	26	5
SN6	19	2	21	27
SN7	20	1	26	1
SN8	21	1	27	16
SN9	26	6	24	72
SN10	20	1	20	92
SN11	17	1		
SN12	26	1		
SN13	22	1		
SN14	22	5		
SN15	16	2		
SN16	20	3		
SN17	21	1		

Three groups of 47 $\mu\text{F}/20\text{ V}$ capacitors were tested at different 3SCT conditions. The first group had 10 cycles per step and voltage increment $\Delta V = 2\text{ V}$; the second was tested at 100 cycles per step and $\Delta V = 1\text{ V}$; and the third also had 100 cycles-per-step, but 2 V increments. Results of testing are displayed in Table 5. The first and the third groups had relatively large proportions of the first cycle failures (77% and 50%), whereas only 33% of parts failed during the first cycle in the second group. This indicates that the proportion of first cycle failures increases with the voltage increment. The majority of the parts in the second group (55%) had N_f exceeding 10.

Table 5. Results of 3SCT at 10 and 100 cycles per step for 47 μ F/20V capacitors.

	10 cycles in 2V incr.		100 cycles in 1V incr.		100 cycles in 2V incr.	
	V _{BR_3SCT}	cycle	V _{BR_3SCT}	cycle	V _{BR_3SCT}	cycle
SN1	52	1	47	51	32	10
SN2	60	1	35	1	44	1
SN3	48	1	53	77	38	1
SN4	50	2	50	5	46	4
SN5	54	9	57	43	42	1
SN6	52	1	48	1	38	2
SN7	50	1	48	25		
SN8	38	4	52	82		
SN9	52	1	56	1		
SN10	50	1				
SN11	24	1				
SN12	26	1				
SN13	52	1				

Table 6 shows failure conditions for two groups of 330 μ F/10 V capacitors tested at 10- and 100-cycle-per-step 3SCT in 1 V increments. Most parts failed after the first cycle during 10-cycle test, but only 33% of parts had $N_f = 1$ during 100-cycle test. Seven out of 18 parts (39%) failed at $N_f > 10$, also without correlation with the breakdown voltage.

Table 6. Results of 3SCT at 10 and 100 cycles per step for 330 μ F/10 V capacitors.

	10 cycles in 1V incr.		100 cycles in 1V incr.	
	V _{BR_3SCT}	cycle	V _{BR_3SCT}	cycle
SN1	11	1	12	66
SN2	11	1	12	9
SN3	10	2	14	6
SN4	11	1	12	10
SN5	10	1	13	11
SN6	9	1	12	1
SN7	11	1	10	3
SN8	9	1	13	1
SN9	11	1	12	1
SN10	10	1	11	1
SN11	12	2	14	35
SN12			12	45
SN13			12	2
SN14			13	58
SN15			15	1
SN16			10	33
SN17			13	37
SN18			17	1

Results of 10- and 100-cycle 3SCT for two groups of 100 μ F/16 V capacitors tested in 1 V increments are shown in Table 7. A large proportion of the parts (30%) failed 100-cycle 3SCT after 10 cycles. Similar to results obtained for other part types, the majority (75%) of 100 μ F/16 V capacitors failed first cycle when subjected to the 10-cycle-per-step testing, whereas only 30% failed first cycle during the 100-cycle testing. This can be explained assuming that the parts failing 100-cycle test after 10 cycles would fail most likely first cycle at the next voltage step during 10-cycle 3SCT.

Table 7. Results of 3SCT at 100 cycles per step for 100 μ F/16 V capacitors.

	10 cycles in 1V incr.		100 cycles in 1V incr.	
	V _{BR_3SCT}	cycle	V _{BR_3SCT}	cycle
SN1	35	1	24	2
SN2	29	10	31	1
SN3	32	1	31	43
SN4	29	1	38	1
SN5	28	1	29	1
SN6	25	1	33	62
SN7	31	1	32	3
SN8	32	1	34	65
SN9	27	3	28	3
SN10	29	1	32	2
SN11	25	1		
SN12	38	7		

To analyze the correlation between the breakdown voltages and the number of cycles-to-failure, the number of cycle-to-failure obtained during 1 V increment, 100-cycle 3SCT were plotted against the normalized breakdown voltage, V_{BR_3SCT}/VR, in Figure 4. The data clearly indicate an absence of correlation between N_f and VBR. Out of 55 samples tested at 100-cycle-per-step, 1 V increment 3SCT, 53% failed after 10 cycles.

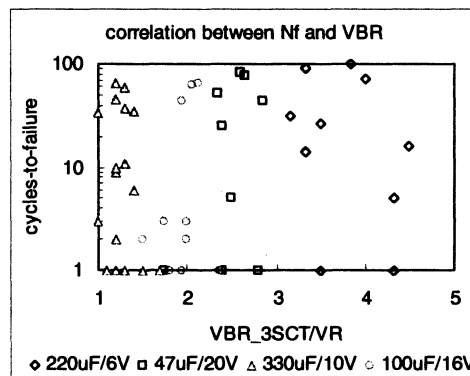


Figure 4. Correlation between the number of cycle-to-failure and breakdown voltage rated to VR during 100-cycle 3SCT in 1 V increment for 220 μ F/6 V, 47 μ F/20 V, 330 μ F/10 V, and 100 μ F/16 V capacitors.

The data for 330 μ F/10 V parts show that even at the rated voltage, failures after more that 10 cycles do happen. For other part types failures at V_{BR_3SCT} = VR were not observed due to much higher characteristic breakdown voltages and respectively much lower probability of failures at VR. However, the absence of N_f -V_{BR_3SCT} correlation allows the assumption that a relatively large proportion of parts failing at VR might fail at N_f exceeding 10 cycles. This means that post-screening failures are possible, and the lower the characteristic breakdown voltage, the greater the probability of these failures.

Statistical data for breakdown voltages measured during 3SCT at 1-, 10-, and 100-cycle-per-step for different part types are summarized in Table 8. It was expected that increased numbers of cycles per step, N_c, would decrease the breakdown voltage. However, the data do not indicate any trend in variation of V_{BR_3SCT} with N_c. This is likely due to the relatively large spread of the breakdown voltages and the small number of tested samples. For 47 μ F/20 V and 22 μ F/35 V parts, the breakdown voltages appear to increase with the number of cycles. However, statistical analysis showed that at the confidence level of 95%, an increase of V_{BR_3SCT} can be confirmed for 47 μ F/20 V parts when comparing 1-cycle and 100-cycle tests only.

Table 8. Effect of number of cycles during 3SCT on breakdown voltages.

part	1 cycle			10 cycles			100 cycles		
	QTY	Average	STD	QTY	Average	STD	QTY	Average	STD
330 μ F 10 V	26	10.8	1.68	11	9.64	0.99	22	11.16	2.34
220 μ F 6 V	36	19.85	4.52	28	19.91	2.78	25	17.35	5.05
47 μ F 20 V	65	40.15	8.87	14	43.84	10.13	9	48.77	6.82
100 μ F 16 V	43	27.8	6.24	19	26.13	5.6	16	26.75	6.13
22 μ F 35 V	33	57.94	11.12	18	62.99	9.29			

It is conceivable that some hardening of the parts occurs during multiple surge current cycling, causing an increase of breakdown voltages. Results obtained by Franklin [4] also indicate that surge testing at lower stress levels can clear some of the faults and improve quality of the parts. Our data show that there is no significant difference in V_{BR_3SCT} between results obtained at different numbers of cycles per step testing. It is possible that both trends, clearing of some faults and damage accumulation, resulting in decrease of V_{BR_3SCT} , coexist resulting in a complex $N_f(V_{BR})$ relationship. Additional analysis is necessary to evaluate the effect of N_c on the surge current breakdown voltages more accurately.

VI. Discussion.

As 100-cycle 3SCT experiments showed, a large proportion of parts in different lots can withstand more than 1,000 cycles (up to 20 100-cycle steps in 1V increment) at voltages gradually increasing from the rated one. Considering possible accelerating factors of the increased stress voltages, it is reasonable to assume that at rated voltages these parts would be able to withstand more than hundreds of thousands of cycles. This means that tantalum capacitors can sustain a practically unlimited number of surge current cycles at low enough voltages. Given that most lots had characteristic breakdown voltages much greater than the rated one, it is possible that the majority of parts in such lots would never fail at the rated voltage. This is consistent with results reported by many authors and implies the existence of a certain threshold voltage, V_{th} , below which surge current failures do not occur.

All parts failing 100-cycle 3SCT at a certain breakdown voltage could withstand more than 100 cycles at a voltage that only 1 V less than the breakdown one. This indicates that there is a relatively narrow range of voltages above V_{th} , at which parts are failing and this range is specific for each capacitor.

A large proportion of parts fail after more than 10 surge cycles, and the number of cycles to failure does not correlate with the breakdown voltage. This casts some doubt upon the common perception that if a part does not fail during the first several surge current cycles, it will never fail under an increased number of cycles. This also impedes the credibility of the existing screening procedure and indicates the possibility of post-screening failures. The probability of failures at $N_f > 10$ is likely to decrease substantially as the test voltage decreases, but for some lots it might be unacceptably high. Considering dramatic consequences of failures of tantalum capacitors in high-reliability applications, this probability cannot be neglected without assessment. Also, the possibility of post-SCT-screening failures requires evaluation of the effectiveness of the screening conditions.

To explain experimental data, assess the probability of surge current failures, and evaluate the effectiveness of SCT screening, a model of surge current failures has been developed.

VI.1. Modeling of the number of cycles to failure.

The suggested model is based on the following assumptions:

1. For each part there is a minimal, critical voltage, V_{cr} , at which the part fails after the first surge current cycle.
2. There is also a certain threshold voltage, V_{th} , below which the part would never fail.
3. At voltages between V_{th} and V_{cr} the part might fail at any number of cycles, N_f , and this number is increasing at voltages closer to V_{th} .
4. Failures at $N_f > 1$ are due to accumulated damage caused by the previous cycles and the failure condition is determined by Miner's rule:

$$N_f \times D = 1, \quad (1)$$

where D is damage produced by one surge current cycle.

5. The value of damage depends on the difference between the stress voltage and V_{th} according to a power law:

$$D = A(V - V_{th})^n, \quad (2)$$

where A and n are constants.

Combining Eq. (1) and (2) N_f can be expressed as follows:

$$N_f = \frac{1}{A \times (V - V_{th})^n}, \quad (3)$$

Assuming that the value of $(V - V_{th})$ represents the damage-inducing stress in the part, equation (3) can be considered similar to the empiric Coffin-Manson model for failures in components and materials induced by mechanical stress cycling. The applicability of this model can be justified assuming that the surge current failures are due to mechanical shocks developed in the part during surge current events. For the Coffin-Manson model, parameter n is typically close to 2, so by adopting this model it can be assumed also that in Eq.(3) $n = 2$.

Considering that at $V = V_{cr}$, $N_f = 1$, constant A can be determined from Eq.(3):

$$A = \frac{1}{(V_{cr} - V_{th})^n}, \quad (4)$$

In this case, the number of cycles to failure can be expressed as follows:

$$N_f = \left(\frac{V_{cr} - V_{th}}{V - V_{th}} \right)^n, \quad (5)$$

Note that V_{th} is less than V_{cr} . This allows expressing the threshold voltage as a portion, α , of the critical voltage:

$$V_{th} = \alpha \times V_{cr}, \quad (6)$$

where $\alpha < 1$.

Using parameter α , Eq.(5) can be simplified and written in the following form:

$$N_f = \left(\frac{1 - \alpha}{V/V_{cr} - \alpha} \right)^n, \quad (7)$$

Obviously, at $V/V_{cr} \leq \alpha$ no failures occur and at $V \geq V_{cr}$ surge current failures would occur during the first test cycle. Considering a relatively narrow range of voltages, where surge current failures were observed, parameter α is likely to vary in a range from 0.8 to 1.

Analysis of variations of N_f with the test voltage at different values of α indicate that even relatively minor variations in α can cause significant changes in N_f and, more importantly, change the minimal voltage above which surge current failures might occur. Parameter α indicates the range of voltages, in which the part can fail after a number of cycles, and together with V_{cr} determines the "never fail" and the first-cycle-failure conditions.

The values of V_{cr} can be obtained experimentally during one-cycle 3SCT with a small voltage increment. Considering that for a given lot, the distribution of V_{cr} is described using a Weibull function with a characteristic breakdown voltage η and shape parameter β , the value of V_{cr} can be expressed via the probability, p, of the part to have $V \leq V_{cr}$:

$$V_{cr} = \eta \times [-\ln(1 - p)]^{1/\beta}, \quad (8)$$

This allows for numerical modeling (Monte Carlo simulation) of the probability of a part to fail after a certain number of cycles. By setting random values of the probability p, $0 < p < 1$, a group of samples having individual values of V_{cr} can be generated using Eq.(8). Then for each sample a number of cycles to failure can be calculated using Eq.(7) for a

range of stress voltages $\alpha V_{cr} < V < V_{cr}$. For voltages outside this range, we assume $N_f = 1$ at $V \geq V_{cr}$, and $N_f = \infty$ at $V < \alpha V_{cr}$.

VI.2. 3SCT simulation.

Using a concept described in the previous section, a Visual Basic program to simulate 3SCT has been developed. The damage after each step prior to failure was calculated as a ratio of the number of cycles at each step, N_c , to the number of cycles to failure, N_f , $D_i = N_c/N_{f,i}$. The accumulated damage was a sum of the step damages:

$$D = \sum D_i = \sum_i \frac{N_c}{N_{f,i}} \quad (9)$$

where

$$N_{f,i} = (1 - D) \times N_f \quad (10)$$

As soon as the condition $N_{f,i} < N_c$ is satisfied, the virtual testing stopped and the program recorded the breakdown voltage, VBR_{3SCT} , equal to the last voltage step, and the number of cycles to failure at this step, N_f .

Experimental data suggest that a proportion of the parts failing the first cycle substantially decreases as the number of cycles during 3SCT increases from 10 to 100. To evaluate the model and estimate its parameters, 3SCT was simulated at $N_c = 10$ and $N_c = 100$ by generating 100 virtual samples at $\eta/VR = 2$, $\beta = 5$, and voltage increment, $\Delta V/VR = 0.1$. Figure 5 shows variation of the proportion of the first-cycle failures with the number of cycles calculated at different parameters α . Comparing these results with experimental data indicates a reasonable agreement at α in the range from 0.9 to 0.95. Distributions of the breakdown voltages calculated during 3SCT simulations at different N_c failed to indicate any trend in the variation of breakdown voltages with the number of cycles, which is also consistent with experimental observations.

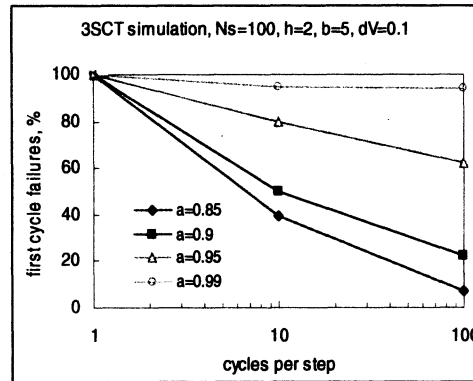


Figure 5. Variation of the proportion of parts failing the first cycle during 3SCT with the number of cycles per step calculated for parts having a Weibull distribution of V_{cr} with parameters $\eta/VR = 2$ and $\beta = 5$.

Another experimental observation is a substantial increase of the proportion of first-cycle failures, $N1$, during 3SCT as the voltage increment increases. Figure 6 shows variations of $N1$ and the probability of parts to fail at the number of cycles more than 10, $N11$, with α at $\Delta V/VR = 0.05$ and 0.1 . The results indicate that at $\alpha = 0.9$, $N1$ increases from 7% at $\Delta V/VR = 0.05$ to 22% at $\Delta V/VR = 0.1$ and the proportion of parts failing after 10 cycles decreases from 70% at $\Delta V/VR = 0.05$ to 24% at $\Delta V/VR = 0.1$. This is also in reasonable agreement with the experimental data.

Figure 7 shows correlation between the 100-cycle 3SCT breakdown voltages and N_f calculated for 20 samples from the lot having $\beta = 5$ and $\eta/VR = 2$. A comparison with Figure 4 shows that for α in the range from 0.85 to 0.95 the results are similar, whereas calculations at $\alpha = 0.99$ resulted in a much higher proportion of the first-cycle failures compared to the experimental data.

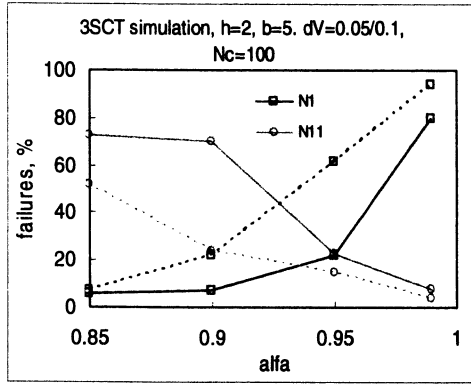


Figure 6. First-cycle failures (N1) and failures after 10 surge cycles (N11) during 3SCT simulations at $0.85 < \alpha < 0.99$ and voltage increments of 0.05 (solid lines) and 0.1 (dashed lines).

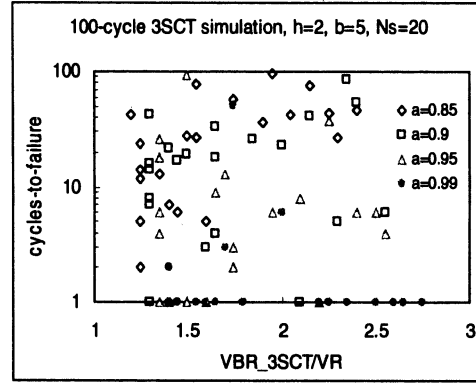


Figure 7. Correlation between the simulated 3SCT breakdown voltages and number of cycles to failure.

VI.3. Screening simulation.

Using Monte Carlo simulations, proportions of parts having first-cycle failures, N_{f1} , parts failing between the first and tenth cycle, N_{f1-10} , parts failing after 10 cycles, N_{f11} , and “never fail” parts, N_g , were calculated for different η/VR and β values. Obviously, $N_{f1} + N_{f1-10}$ is the proportion of screening failures and N_{f11} is the proportion of post-screening failures. The purpose of separating N_{f1} and N_{f1-10} is to estimate the proportion of first-cycle failures compared to the total number of screening failures. This simulation was carried out by generating 1,000,000 virtual samples having Weibull distribution of V_{cr} with $1 < \eta/VR < 4$ and $\beta = 5$ and 10. Results of these calculations at $\alpha = 0.9$ and $\alpha = 0.99$ are shown in Figure 8.

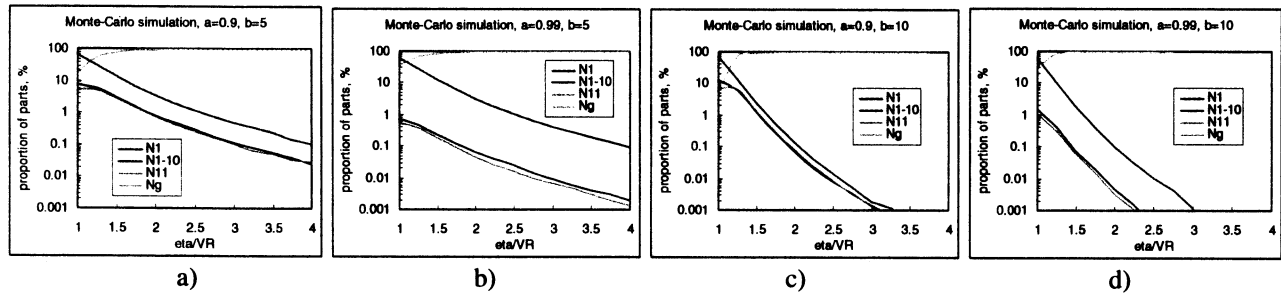


Figure 8. Calculated proportion of parts failing at $V = VR$ after the first cycle (N1), from the first to tenth cycles (N1-10), and after the tenth cycle (N11) at different parameters of the model Eq. (6, 7). N_g indicates a proportion of good, “never failed” parts. The data were calculated for $\beta = 5$ (a, b); $\beta = 10$ (c, d); and $\alpha = 0.9$ (a, c), $\alpha = 0.99$ (b, d).

Analysis shows a sharp, near-exponential decrease of the probability of surge current failures with η exceeding 1.5. A similar effect has an increase of the shape parameter: at $\eta/VR = 2$ and $\alpha = 0.9$, a proportion of parts failing SCT decreases from 1.9% to 0.01% as β increases from 4 to 14. At $\alpha = 0.99$ this decrease is even more substantial, from 0.16% at $\beta = 4$ to $6.1E-4\%$ at $\beta = 14$.

For typical cases of lots having $\eta/VR = 2.5$ and $\beta = 5$ and 10, the proportion of screening (10 cycles at VR) failures and post-screening failures at the rated voltage were calculated. The first-cycle failures at VR comprise the majority (from 67% to 94%) of all screening failures, which is typically observed during SCT screening. The proportion of post-screening failures is from 3 to 6 times to 66 to 550 times less than the proportion of screening failures, for $\alpha = 0.9$ and $\alpha = 0.99$ respectively. A generally low probability of screening failures and even lower probability of post-screening failures could explain the common perception that if a part does not fail during the first few cycles, it never fails at a greater number of cycles.

Figure 9 shows variations of the probability of post-screening failures with parameters of Weibull distributions and α in the range from 0.85 to 0.95. These calculations imitate regular, 10-cycle screening at rated voltages. At relatively small shape factors, $\beta < 5$, and characteristic breakdown voltages, $\eta/VR < 2$, the probability of post-screening failures exceeds 0.2%, which is not acceptable for high-reliability applications. For a typical case with $\eta/VR = 2$ and $\beta = 8$, the model predicts that from 0.07% to 0.5% of parts might fail if surge current events at the rated voltage happen after screening. Obviously, the probability of failing first cycle after screening is much lower, but in many cases is not negligible.

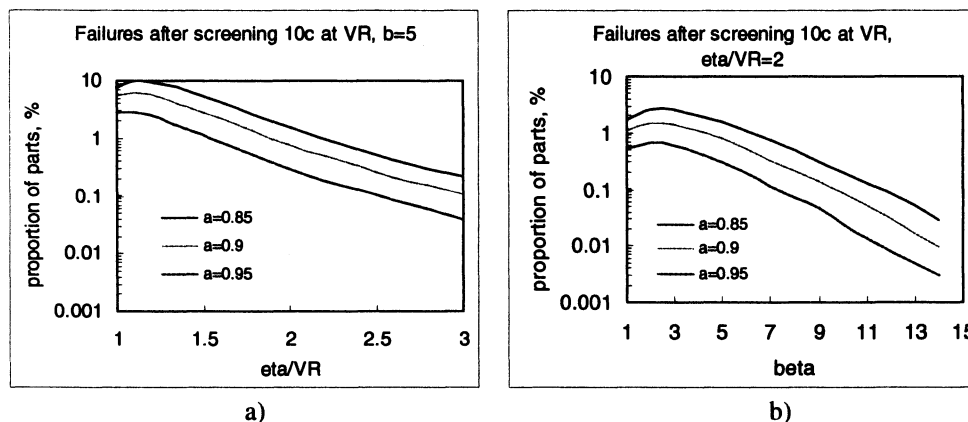


Figure 9. Probability of post-screening failures at different parameters of Weibull distributions and α . Screening simulation: 10 cycles at the rated voltage.

To reduce the probability of failures during applications, surge current screening should be performed at voltages exceeding the rated ones. Analysis of the model shows that by increasing screening voltage to $V_{scr} = VR/\alpha$, the majority of post-screening failures can be eliminated. Considering that the most probable range of α is from 0.85 to 0.95, screening should be performed at voltages 1.1VR to 1.15VR. It should be noted that AVX is routinely performing SCT screening at 1.1VR during manufacturing of their products [13]. This indicates that this test condition is quite realistic, and the requirement for tantalum capacitors to sustain surge current testing at voltages exceeding VR should be included in the relevant specifications for parts used in military and space applications.

VII. Conclusion.

1. Life testing of 5 part types at 125 °C and $V = 1.5VR$ for up to 250 hours resulted in a statistically significant number of failures, but no differences in the test results between the SCT-screened and non-screened groups were observed. Additionally, four part types were tested at room temperature and 2VR for 200 hours, while leakage currents were monitored to record scintillation events (failures). Similar to life testing at 125 °C, statistical analysis showed no difference in the proportion of failures in groups with and without SCT screening.
2. To evaluate the effect of Weibull grading on surge current breakdown voltages, 3SCT was carried out on parts after life testing. Analysis showed no significant effect of the life testing at 125 °C; however, room temperature long-term stress of the parts at high voltages increased surge current breakdown voltages on 10% to 20%.
3. Results obtained for the SCT-screened and non-screened parts before and after life testing showed that SCT screening was not a significant factor of life testing. Also, the life test did not degrade surge current breakdown voltages. For this reason, options B and C per MIL-PRF-55365 can be considered as equivalent.
4. Results of SCT with multiple cycling at different voltages showed no evidence of degradation even at voltages close to the breakdown, and indicated that at relatively low voltages solid tantalum capacitors can withstand a practically unlimited number of high-current cycles with amplitudes exceeding hundred amperes. This suggests that there is a certain threshold voltage, V_{th} , below which surge current failures do not occur.
5. The results of 3SCT with multiple cycles per step showed that the parts can fail at any number of cycles, N_f , which apparently randomly varies from 1 to 100 without correlation with the breakdown voltage. A relatively large proportion of parts, 53% out of 55 samples tested at 100 cycles per step and 1 V increments, failed after 10 cycles.

6. A model of surge current failures allowing calculations of the number of cycles to failure for a given distribution of V_{cr} (a minimum voltage resulting in surge current failure at the first cycle), has been developed. Simulation of 3SCT using Eq.(7) and (8) showed a reasonable agreement with the experimental data at the model parameters α in the range from 0.85 to 0.95 and $n = 2$. At relatively small shape factors, $\beta < 5$, and characteristic breakdown voltages, $\eta/VR < 2$, the model predicted a rather high probability of post-screening failures exceeding 0.2%.
7. To reduce the probability of failures during applications, surge current screening should be performed at voltages exceeding the rated ones. Analysis shows that by increasing screening voltage to 1.15VR, the majority of post-screening failures at the rated voltage can be eliminated. The results of experiments show that these screening conditions do not degrade quality and reliability of chip tantalum capacitors.

VIII. Acknowledgement.

This work was sponsored by the NASA Electronic Parts and Packaging (NEPP) program. The author is thankful to Michel Sampson, NEPP program manager, who recognized the need of this investigation and to Jeanne Beatty for editing the manuscript.

IX. References.

- [1] M. J. Cozzolino and R. C. Straessle, "Design, characteristics, and failure mechanisms of tantalum capacitors," Proceedings of 8th CARTS'88, San Diego, CA, 1988, pp. 98-110.
- [2] K. Lai, E. Chen, P. Blais, P. Lessner, B. Long, A. Mayer, and J. Prymak, "Step Surge Stress Test (SSST) Defines Dielectric Capability," Proceedings of CARTS in Asia, Taiwan, 2007, pp.
- [3] J. D. Prymak, "Performance issues for polymer cathodes in Al and Ta capacitors," Proceedings of CARTS USA 2001, 2001, pp. 25-34.
- [4] R. W. Franklin, "Surge current testing of resin dipped tantalum capacitors," *AVX technical information*, 1985. <http://www.avxcorp.com/docs/techinfo/dipptant.pdf>.
- [5] H. W. Holland, "Effect of high current transients on solid tantalum capacitors," *KEMET Engineering bulletin*, 1996.
- [6] D. Mattingly, "Increasing reliability of SMD tantalum capacitors in low impedance applications," *AVX technical information*, 1995. <http://www.avxcorp.com/docs/techinfo/tantimp.pdf>.
- [7] J. Gill, "Surge in solid tantalum capacitors," *AVX Technical information*, 1995. <http://www.avxcorp.com/docs/techinfo/surgtant.pdf>.
- [8] B. S. Mogilevsky, G., "Surge Current Failure in Solid Electrolyte Tantalum Capacitors," *IEEE Transactions on Components, Hybrids, and Manufacturing Technology*, vol. 9, pp. 475 - 479, 1986.
- [9] P. Fagerholt, "A new view on failure phenomena in solid tantalum capacitors," Proceedings of 16th Capacitors and Resistors Technology Symposium, CARTS'96, 1996, pp. 162-166.
- [10] J. D. Prymak, "Derating Differences in Tantalum-MnO₂ vs. Tantalum-Polymer vs. Aluminum-Polymer," Proceedings of 23rd Capacitor And Resistor Technology Symposium, 2003, pp. 278-283.
- [11] A. Teverovsky, "Effect of compressive stresses on performance and reliability of chip tantalum capacitors," Proceedings of CARTS Europe, Barcelona, Spain, 2007, pp. 175-190.
- [12] J. D. Moynihan and A. M. Holladay, "Effectiveness of surge current screening of solid tantalum capacitors," Proceedings of CARTS 1983, Phoenix AZ, 1983, pp. 53-60.
- [13] T. Zednicek and J. Gill, "Voltage derating rules for solid tantalum and niobium capacitors," Proceedings of CARTS EUROPE, 2003, pp. 44-50.